A Screening Method Using Pulsed-Power Combined with Infrared Imaging to Detect Pattern Defects in Bulk Metal Foil or Thin Film Resistors

Jay Brusse[(1)], Lyudmyla Panashchenko[(2)]

[1] ASRC AS&D at NASA Goddard Space Flight Center Code 562
Greenbelt, MD 20771 USA
Jay.A.Brusse@nasa.gov

[2] NASA Goddard Space Flight Center Code 562
Greenbelt, MD 20771 USA
Lyudmyla.P@nasa.gov

ABSTRACT

Bulk metal foil and thin film resistors occasionally contain localized defects within the etched resistor pattern. Common defects of this type include in-line constrictions referred to as notches, unremoved resistor material bridges between adjacent pattern lines, and embedded non-conductive particles in the resistor material. Such defects are prone to fracture due to thermomechanical fatigue during powered operation, especially power cycling, resulting in positive resistance change and open circuit failure modes. Common screening methods of optical microscopy, short time overload power tests (e.g., 6.25x rated power for 5 seconds) and burn-in (e.g., 1.5x rated power for 100 hours) are useful, but they are not always effective at removing devices with such defects.

An improved method has been developed to screen for localized resistor pattern defects. The method involves the application of brief, high power electrical pulses at a low duty cycle while inspecting the resistor with a high resolution, high speed infrared camera. The following test conditions were found to be suitable for this purpose: 6.25x rated power, 1 to 5 pulses, 50 ms pulse width and 10% duty cycle. During the power pulsing, localized constrictions in the resistor pattern are identifiable as hot spots via the infrared camera. Reject criteria can be established based on observations of hot spots.

To assess its effectiveness, a total of two hundred eighty (280) surface mount foil resistors (40 each from 7 different lots) were screened using this infrared technique. The screening identified twenty-nine (29) resistors with significant hot spots in the resistor pattern. All 280 resistors were then subjected to an industry standard 10,000 hour life test at 1x rated power at 70°C with power cycled for 90 minutes on and 30 minutes off. During life testing, three resistors exhibited positive resistance change failure mode. All three failures were due to thermomechanical fatigue failure of localized bridge defects at the locations identified via infrared screening. The results of this evaluation illustrate the benefits of the pulsed-power infrared detection screening technique to identify reliability suspect foil or thin film resistors that may escape common screening methods.

INTRODUCTION

Bulk metal foil resistors and thin film resistors are mature technologies that have found broad use in all types of electronic circuit applications including commercial, industrial, military and aerospace sectors. Among the many favorable attributes of these types of resistors are the wide range of resistance values available, tight resistance tolerances (as low as ±0.01%), and long-term stability (as low as ±0.005%) [1, 2]. Foil resistors are especially advantageous for their excellent stability over wide temperature ranges with temperature coefficients of resistance (TCR) of less than 1 ppm/°C available [2].

Occasionally, some resistors are produced having small localized constriction defects (i.e., significant reduction of the cross sectional area) in a current-carrying portion of the serpentine resistor pattern. During powered operation of the resistor, these localized constrictions experience higher current density compared to the non-constricted resistor pattern. The higher current density produces localized hot spots due to increased Joule heating at the site of the defect. These localized hot spots experience higher stresses due to greater thermal expansion of the resistor material at the site of the constriction. Especially during power cycling, the constriction defects may fracture due to thermomechanically-induced cyclical fatigue. Depending on the location of the constriction in the resistor pattern, a fracture will induce a positive resistance shift up to and including an open circuit failure mode.

Traditional screening tests for resistors that might detect localized constriction defects include optical microscopy inspection of the resistor pattern prior to encapsulation or powered tests such as short time overload (STOL) and power conditioning (also known as burn-in) tests such as described in [1 - 3]. Experience has shown that despite the implementation of these screening tests, occasionally, some resistors with localized constriction defects will be supplied [4 - 8].

To be published in the conference proceedings of the Space Passive Component Days (SPCD) international Symposium, Noordwijk, The Netherlands, October 9-12, 2018.

In this report, we will describe a new screening method to detect localized constriction defects in foil and thin film resistor patterns using a high resolution, high speed infrared camera to identify localized hot spots while applying brief duration, power pulses. Furthermore, we will describe a long-term life test evaluation to assess the effectiveness of this new technique to screen out reliability suspect resistors thereby enhancing reliability.

BULK METAL FOIL RESISTOR CONSTRUCTION

Surface mount foil resistors are commonly produced as two terminal devices with solderable wraparound terminations. They are available in a variety of standard footprints including sizes 0603 up to 2512 (see Fig. 1a). The basic construction of a bulk metal foil resistor is described in several patents [9, 10] and illustrated in Fig. 1 and Fig. 2 [7]. The typical surface mount foil resistor consists of a flat, rectangular, insulating substrate (e.g., alumina) on top of which the resistor element is bonded using adhesive materials (e.g., resins or polymers). The resistor element is made from proprietary nickel-chromium based alloy ingots that are precision-rolled into foil sheets having thicknesses in the range from ~2 μm to ~5 μm. The foil sheets are then developed into serpentine resistor patterns using photolithography and electrochemical etching techniques. A wide assortment of resistor patterns may be produced with individual patterns having resistor lines (also called "gridlines") having widths ranging from a few microns to many tens of microns depending on the resistance values to be achieved from that pattern. Fig. 1b and 1c provide examples of the serpentine resistor patterns for a low value (49.9 Ω) vs. high value (20,000 Ω) resistor each produced on a size 1206 alumina substrate.

The resistor pattern is comprised of a non-adjustable resistor section(s) plus a plurality of sections of various resistance values where each additional section has its own removable shorting tab connected to it in parallel. The removal of a shorting tab (process known as trimming) is performed by the manufacturer using laser cutting, mechanical scribing or micro-sandblasting techniques. Removal of a shorting tab connects the associated previously-shorted resistor section in series with the remainder of the pattern thereby increasing the total resistance of the pattern by a fixed amount. By removing various combinations of shorting tabs, the resistor can be trimmed to any desired resistance value within a broad range and also achieve very precise tolerances (e.g., ±0.01%).

The resistor element is protected by a thin (~5 μm to ~10 μm), optically translucent polymeric coating followed by a thin (~25 μm), optically opaque epoxy coating to protect the resistor element against handling damage and to allow for the printing of part markings (e.g., lot date code) onto the external surface of the component (see Fig. 2).

a)

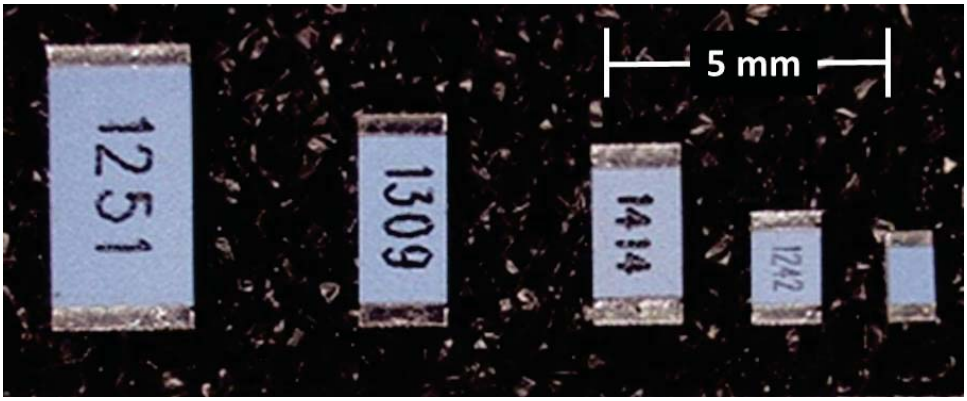

b)

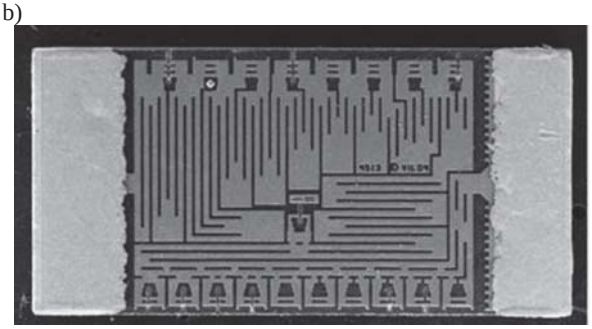

c)

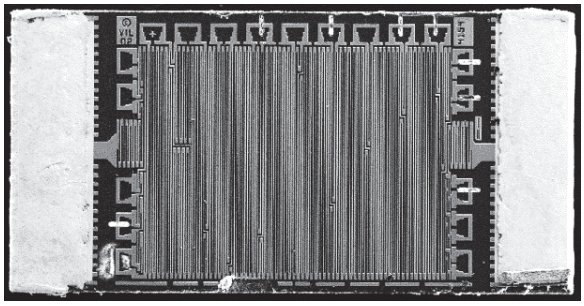

Fig. 1. a) Surface Mount Foil Resistors Sizes 2010 to 0603
Etched foil resistor pattern for size 1206 surface mount foil resistors b) 49.9 Ω and c) 20,000 Ω

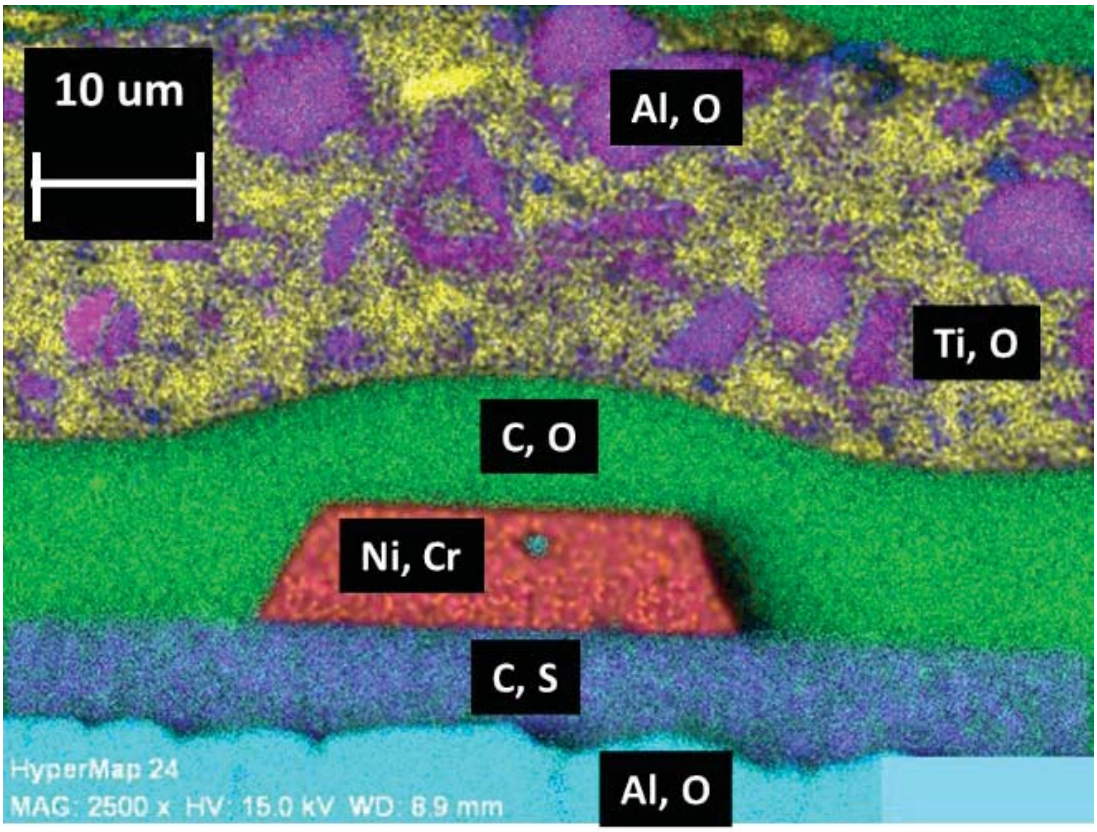

Fig. 2. Scanning Electron Microscopy (SEM) Image with Elemental Dot Map of a Cross Section of a Typical Surface Mount Foil Resistor

CONSTRICTION DEFECTS IN FOIL RESISTOR PATTERNS

Two main types of constriction defects may occur during the manufacturing of the foil resistor element: notches and bridges. Examples of each type of constriction defect are shown in Fig. 3 [4 - 8].

Notch defects are localized holes in the resistor gridline that reduce the gridline cross sectional area below the original design intent. Notches that take away >75% of the nominal resistor line width are considered to be unacceptable by some workmanship inspection criteria [3, 11] when the pattern is inspected at 30x magnification. The causes of notch defects include pre-existing pin holes in the foil sheet prior to etching, photolithography/etching-related anomalies and non-conductive particles (e.g., aluminum nitride) embedded in the foil [5]. If a notch defect breaks, then the electrical continuity of the gridline pattern is interrupted usually resulting in an open circuit failure mode. If the disrupted section of the resistor pattern has an associated parallel pathway, then a positive resistance shift occurs.

Bridge defects, as the name suggests, are sections of foil resistor material that interconnect two or more adjacent gridlines. Bridges whose narrowest width is <10% of the nominal resistor line width are considered to be unacceptable [3, 11]. The primary causes of bridge defects are related to photolithography/etching anomalies that result in a failure to completely remove foil material from the spaces between adjacent lines as intended. Bridges form unintentional parallel resistor pathways within the serpentine pattern. If during the trimming operation the manufacturer cuts a shorting tab associated with a section of the pattern containing bridge defects, then these bridges and the parallel resistance pathways they produce become essential features of the overall resistance value. Any disruption of the bridge would result in removal of the parallel path and an associated increase in resistance value.

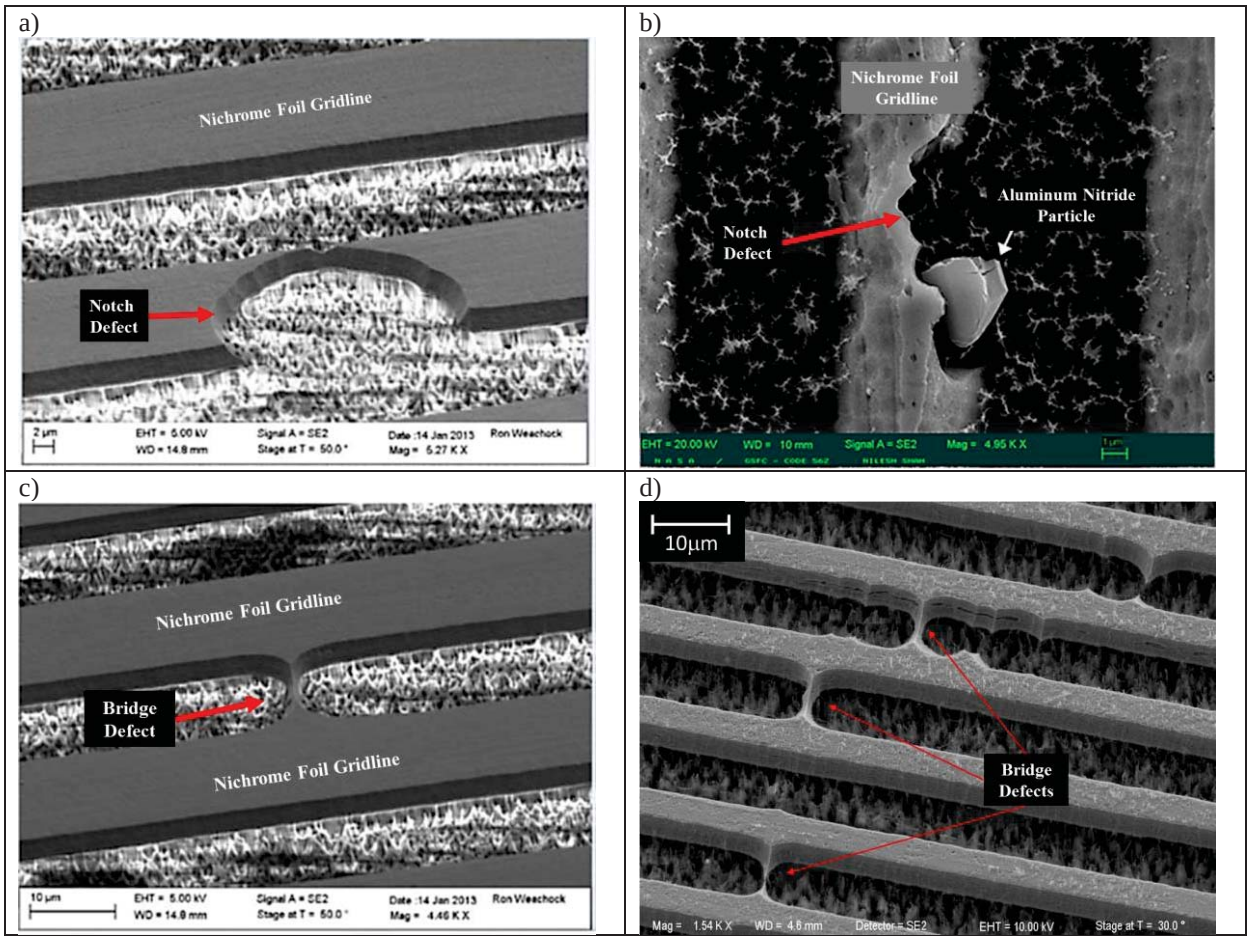

Fig 3. Destructive Physical Analysis (DPA) Examples of Constriction Defects in Foil Resistors
a) Large Notch Defect in Gridline,
b) Notch Defect Associated with an Aluminum Nitride Particle Embedded in the Foil,
c) and d) Bridge Defects Between Adjacent Gridlines

TRADITIONAL SCREENING METHODS TO DETECT CONSTRICTION DEFECTS

The techniques listed in Table 1 and further described in [1 – 3, 11] are sometimes used by resistor manufacturers and others to screen individual foil resistors and/or to test samples from a production lot to identify resistors with localized constriction defects in the resistor pattern. Each of these techniques is capable of identifying some number of resistors with constriction defects either by direct optical detection or by inducing mechanical fracture of the constriction. However, occasional field failure experiences and post-procurement destructive physical analysis (DPA) rejections show that these traditional methods still allow some devices with constriction defects to remain in some lots. For example, the images of constriction defects shown previously in Fig. 3 are all from DPAs or failure analyses of resistors that had been screened by some or all of these traditional methods.

Table 1. Traditional Methods Used to Screen Surface Mount Foil Resistors
for Constriction Defects in the Resistor Pattern

Test Name	Test Conditions	Rejection Criteria	Sample Size
Optical Microscopy *Prior to encapsulation*	30x to 60x	Notches >75% of nominal line width Bridges <10% of nominal line width	100% high reliability products only
Short Time Overload (STOL)	6.25x rated power 5 seconds	$\Delta R > 0.02\%$	10% to 100% high reliability products only
Power Conditioning (Burn-In)	1.5x rated power 100 hours @ 70°C	$\Delta R > 0.03\%$	100% high reliability products only
Destructive Physical Analysis (DPA)	MIL-STD-1580 & MIL-PRF-55182	Notches >75% of nominal line width Bridges <10% of nominal line width	3 to 5 resistors per lot

DESCRIPTION OF A NEW PULSED-POWER INFRARED SCREENING TECHNIQUE

With support from the NASA Electronic Parts & Packaging (NEPP) Program the authors have developed a new screening technique for foil and thin film resistors that is intended to augment the traditional testing methods in Table 1. This new technique was initially described in our previous publication [12]. The primary objective of this technique is to identify and remove from the lot any resistors having significant localized constriction defects (notches and/or bridges) within the active region of the resistor pattern. The technique is based upon the principal that significant constrictions will exhibit substantially greater Joule heating during powered operation compared to segments of the resistor pattern with the intended cross sectional area. The increased Joule heating results in the formation of localized hot spots in the resistor pattern which may then be detected by infrared thermography if the infrared detector has sufficient resolution.

The screening technique begins by selecting an appropriate set of power parameters to apply to the resistor under test. The objective is to produce Joule heating that is focused and confined primarily at the sites of localized constriction defects within the active region of the resistor pattern. The authors have found the pulsed-power square wave shown in Fig. 4 to be well-suited for this purpose. A Keysight model B2962A or similar low noise power source may be used. The choice of 6.25x rated power is based upon this same power level having already been established as the industry norm for the 5 second short time overload (STOL) screening test for both foil resistors and thin film resistors [1 – 3]. Obviously, if these resistors are specified to survive the 5 second 6.25x rated power STOL test with no damage, then it is reasonable to expect them to withstand the same power for 1/100th the time (i.e., 50 ms). The brevity of the pulse and 10% duty cycle confines the Joule heating of the localized constrictions to a small distance thereby allowing an infrared detector to provide more accurate location of the hot spot. In practice, only a single pulse is necessary to perform the test, but the authors have found using from 1 to 5 pulses enables a human operator to more easily review and interpret the infrared video captured for the resistor under test. Future improvements of this test may employ software automated interpretation of the infrared images instead of human interpretation.

Power = 6.25x rated power
Pulse Width = 50 ms
Pulse Period = 500 ms (i.e., 10% duty cycle)
# of pulses = 1 to 5

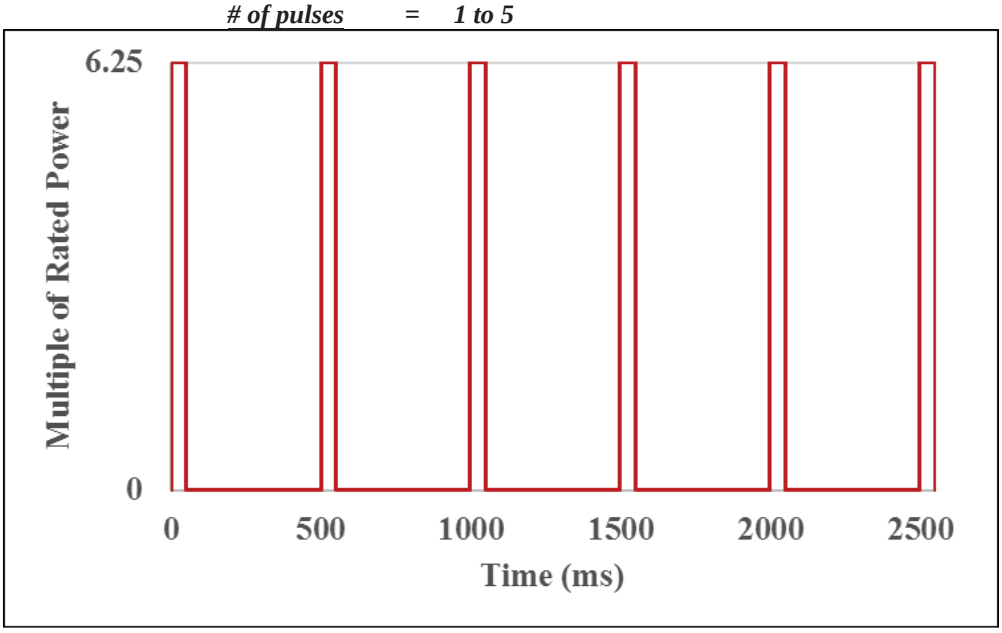

Fig 4. Pulsed-Power Parameters Used for Infrared Screening of Surface Mount Foil Resistors

The key feature of this new screening method is the use of the FLIR SC8300 series high-speed, high-resolution infrared camera combined with a 4x magnifying lens (see Fig. 5) to capture infrared video (i.e., sequence of images) of the resistor pattern while applying the pulsed-power signal of Fig. 4. Relevant specification parameters for this camera and lens configuration are listed in Table 2 and described in [13]. The field of view of ~4.6mm x ~5.6mm enables inspection of resistors up to size 2010 in a single inspection. Larger footprint resistors require 2 or more inspections with repositioning of the sample between inspections in order to examine the entire active area. The detector has over 1 million pixels that can readily detect feature sizes down to ~5 µm which is sufficient to identify hot spots associated with constriction defects found in the etched resistor pattern geometries in production today.

Fig 5. FLIR SC8300 Series Infrared Camera with 4x Lens

Table 2. Specification of selected parameters for the FLIR SC8300 infrared camera with 4x lens

Parameter	Specification
Detector	InSb
Spectral Range	1.5 μm to 5 μm
Measurement Temperature Range	-20°C to +350°C
Field of View	~4.6mm x 5.6mm (> 1 million pixels)
Resolution of Feature Sizes	~ 5 μm per pixel
Working Distance at Focal Plane	~25mm
Frame Capture Rate	>100 frames per second (fps)

In our previous work [12] we first used the pulsed-power infrared inspection technique to examine a resistor that had failed the DPA workmanship criteria. During DPA both the polymer and epoxy coatings over the resistor element were removed. After coating removal, scanning electron microscopy (SEM) inspection identified both a notch and a bridge defect in the active region of the pattern each of which failed the established workmanship criteria in [3, 11] (i.e., notch > 75% of gridline width and bridge < 10% gridline width).

The first pulsed-power infrared inspection for this resistor DPA sample was performed using a FLIR SC660 infrared camera with ~25 μm resolution after which the same resistor was re-examined using the FLIR SC8300 high resolution infrared camera (see Fig. 6).

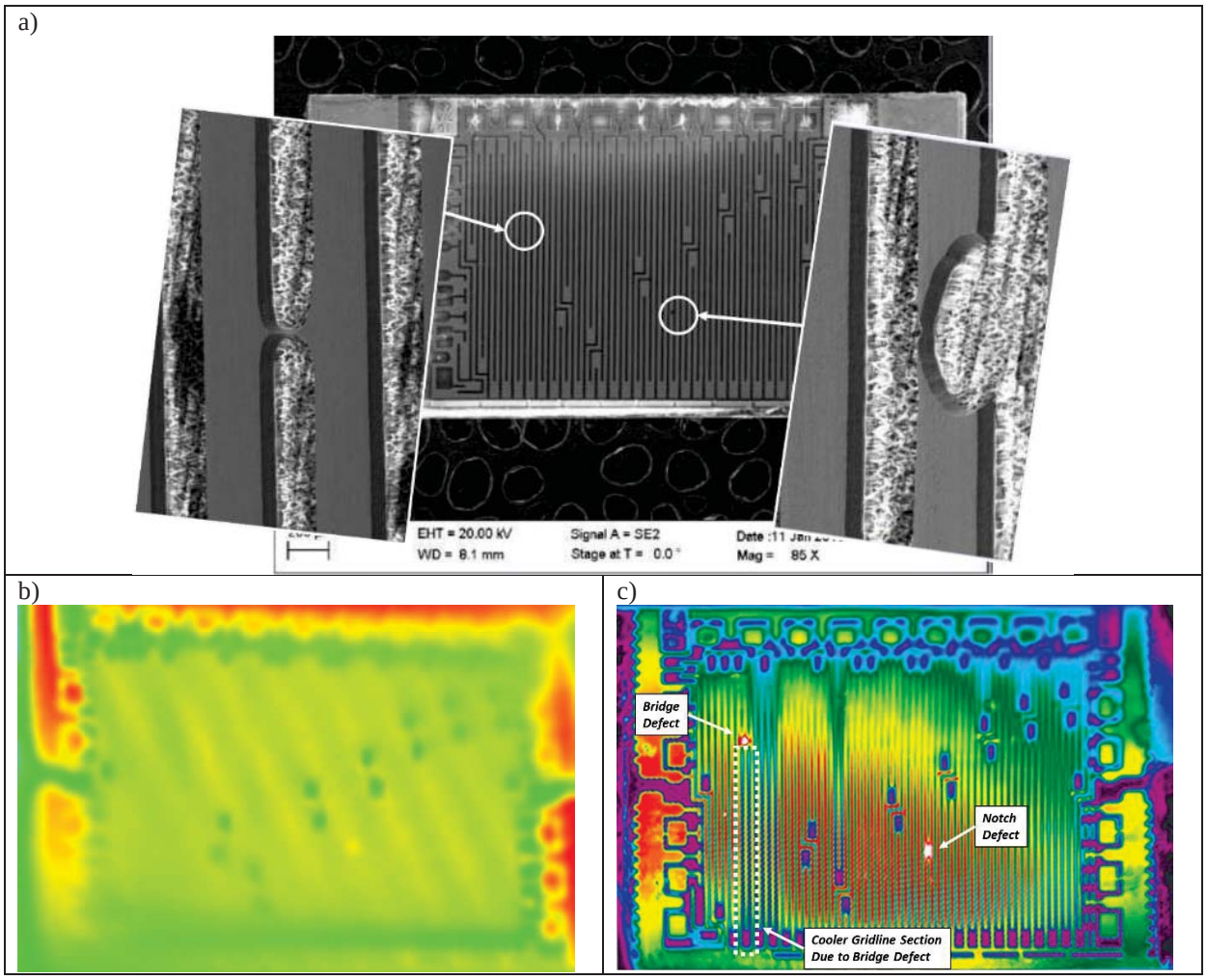

Fig 6. Inspection of a Single DPA Sample Foil Resistor Having 1 Notch and 1 Bridge Defect
a) SEM Images, b) Low Resolution Infrared FLIR SC660, and c) High Resolution Infrared FLIR SC8300

The difference in resolution of the images acquired by the two infrared cameras was remarkable. Hot spots associated with both the notch and bridge defects (seen as white in this color palette) were readily identified by the FLIR SC8300 whereas the same defects were not discernable with the SC660. Even without a-priori knowledge from high-magnification SEM inspection, the high-resolution infrared image can be used to identify the constriction defect type. For example, the notch defect shown in Fig. 6 is revealed as a hot spot contained within a single gridline run. The notch is also identifiable by noting that the temperatures of the gridline runs entering and exiting the notch are approximately the same magnitude since the current flowing in each is the same and therefore, so too is the Joule heating. The bridge defect in Fig. 6 appears as a hot spot between two adjacent gridlines. The bridge can also be recognized by the much cooler temperature of the gridline section beyond the bridge defect where less current is flowing due to the bypass provided by the bridge. These initial results provided the motivation to pursue the use of the FLIR SC8300 as a non-destructive, post-procurement screening inspection tool.

To assess this potential the authors examined several surface mount foil resistors and thin film resistors from more than one source with all of the protective coatings still intact. To our surprise, even with no power applied to the resistor and with the protective polymer and epoxy coatings still present, the FLIR SC8300 camera was able to produce a detailed image of the resistor pattern beneath the coatings almost as if the coatings were not present (see Fig. 7). The SC660 camera could not identify pattern features with the coatings present. Such detail was possible with the SC8300 due to the highly transmissive attributes of these specific protective coatings in the spectral range (~1.5 μm to ~5 μm) used by this infrared detector. Notice in Fig. 7b, however, that the black marking ink used to label the resistor with lot date code information is more opaque in this infrared spectral range. Nevertheless, even with this hindrance, the ability to see through the coatings is highly advantageous for this screening technique.

a) b)

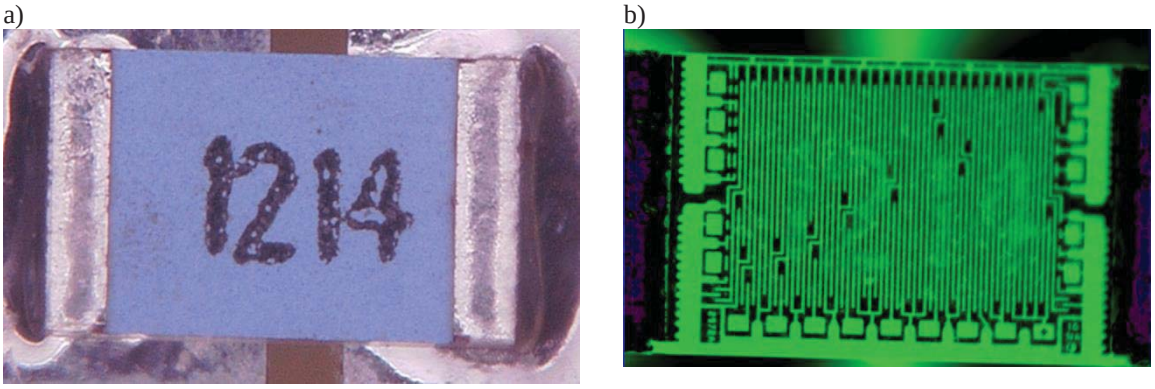

Fig 7. a) Optical Microscopy Image of a Foil Resistor and
b) FLIR SC8300 Infrared Image of Resistor in a) without Removing Protective Coating and Without Power Applied

Next, infrared inspection was performed on several surface mount foil resistors and some surface mount thin film resistors while applying brief power pulses as described in Fig. 4. Fig. 8 provides a few examples of the kinds of pulsed-power infrared images obtained at this stage of development. The infrared camera's software allows selection of a variety of color palettes to represent different temperatures within the field of view. For these images the green palette was chosen where darker colors are cooler and lighter colors are hotter. Note: Due to differences in the emissivity of the marking ink compared to the other materials, the part markings give a false impression of hotter temperatures at their location.

a) b)

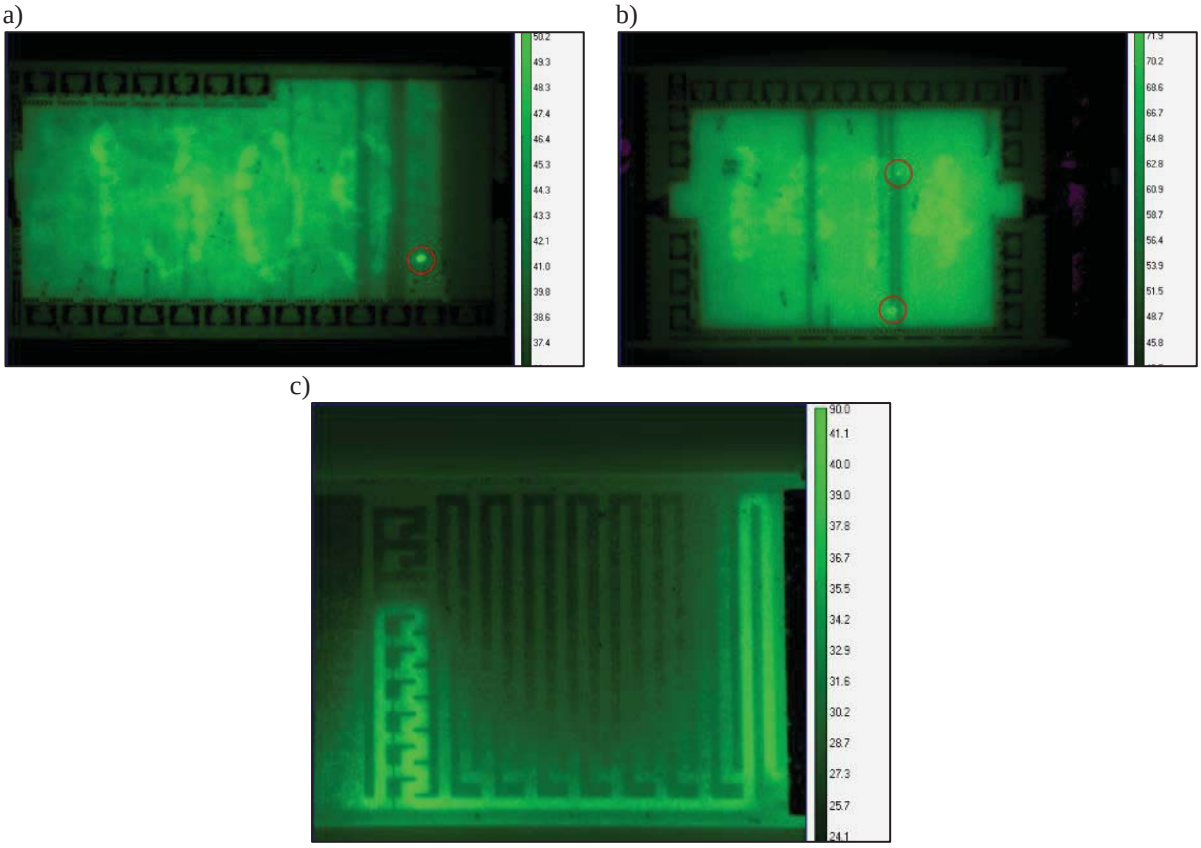

Fig. 8 – Examples of Pulsed-Power Infrared Images of
a) Foil Resistor with a Notch Type Defect, b) Foil Resistor with 2 Bridge Type Defects and
c) Thin Film Resistor with No Defects

EVALATUION OF THE NEW SCREENING METHOD

Having established the feasibility of the pulsed-power infrared screening method described above, an evaluation was performed to determine its effectiveness to non-destructively identify foil resistors having localized constriction defects and furthermore, to assess what, if any, effect such defects have on long-term reliability. The evaluation flow is shown in Fig. 9.

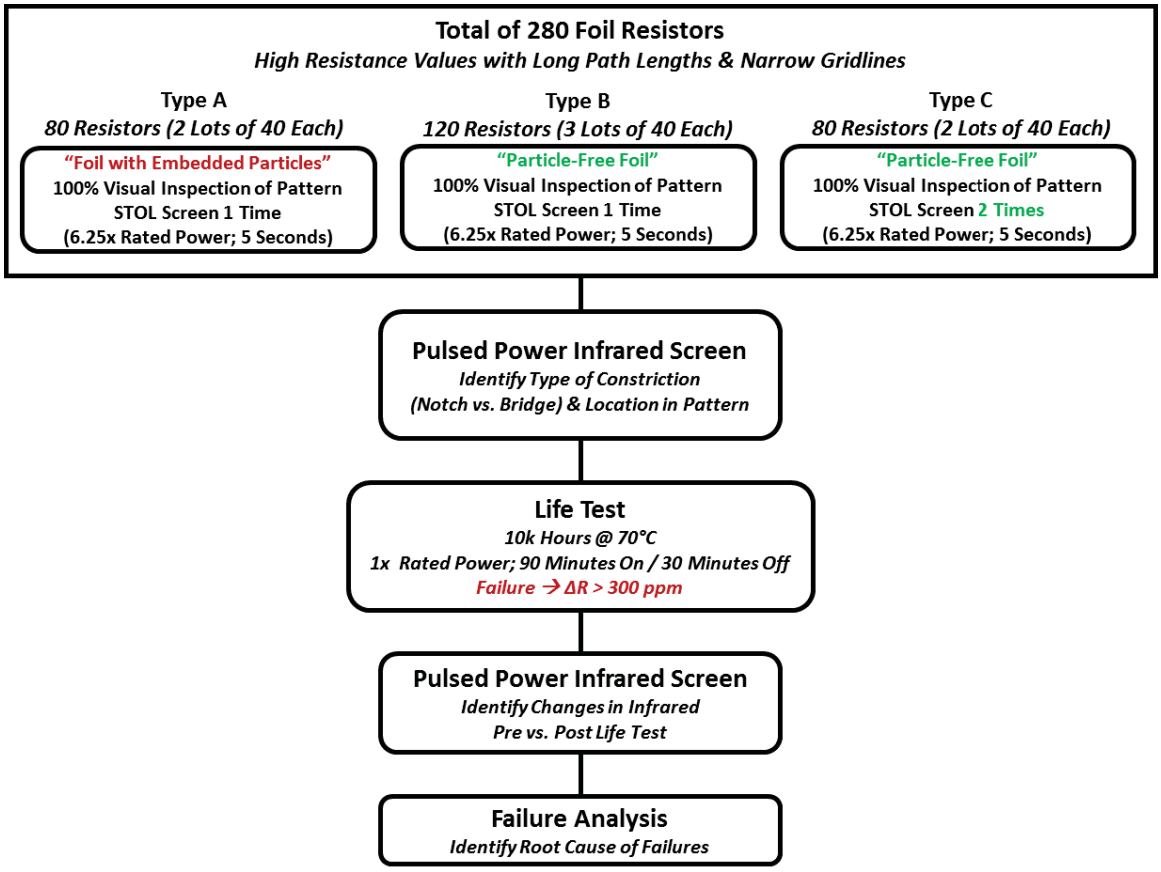

Fig. 9. Evaluation Test Flow Used to Assess Effectiveness of Pulsed-Power Infrared Screening Method

A total of 280 surface mount foil resistors (7 different lots of 40 resistors each) identified in Table 3 were obtained for this evaluation. Each of the 7 lots was chosen to have a high resistance value with small cross section gridlines (e.g., ~4μm to 7μm wide and ~2.5μm thick) and long resistance path lengths which tend to increase the potential for some resistors to have notch or bridge defects whose sizes might result in significant constrictions.

Table 3. Bulk Metal Foil Surface Mount Resistors Used for this Evaluation

Type	Resistor Size (EIA footprint)	Resistance (Ω) & Tolerance	Power Rating (mW)	Lot Date Code	Qty	Resistor Pattern Geometry	
						Foil Thickness (μm)	Foil Line Width (μm)
C	0805	5100 ± 0.05%	100	1242	40	2.3	6.6
A	1206	20000 ± 0.05%	150	1309	40	2.5	4.8
B	1206	20000 ± 0.05%	150	1414	40	2.5	4.8
C	1206	23500 ± 0.05%	150	1420	40	2.3	4.3
A	1506	36450 ± 0.05%	200	1309	40	2.8	4.1
B	1506	36450 ± 0.05%	200	1309	40	2.8	4.1
B	2010	50000 ± 0.01%	300	1251	40	2.5	4.8

Resistors were categorized by three distinct "Types" identified as A, B or C. Using proprietary inspection techniques, the manufacturer determined that resistors from Type A were produced from foil sheet materials having embedded particles (e.g., aluminum nitride) which increases the potential for particle-related gridline constrictions. Contrastingly, resistors from Types B and C were made from so-called "particle-free foil" which is terminology used by the manufacturer to describe foil sheet material having a very low (or zero) concentration of embedded particles and whose particle size distributions are small with respect to most gridlines.

The manufacturer performed an in-process 100% pre-encapsulation visual inspection at ~30x to 60x on the etched resistor patterns to remove resistors having pattern anomalies detectable with this technique. Due to the complexity and extremely small feature sizes of both the gridlines and many of the constriction type defects, this method is expected to allow some resistors with smaller defects to remain in the lot.

Finally, the manufacturer performed the industry standard 5 second STOL test [1 – 3] one time on resistors from Types A and B and performed STOL testing two times on resistors from Type C. With the STOL test the resistor manufacturer intends to screen out resistors having the narrowest constriction defects in the active region ostensibly by fracturing (or melting) the constriction and then detecting this fracture as a positive resistance change or open circuit failure after STOL.

RESULTS OF THE EVALUATION

Pre-Life Test Pulsed-Power Infrared Screening Results

A total of 280 resistors identified in Table 3 were screened prior to life test using the aforementioned pulsed-power infrared inspection technique in Fig. 4. A serialization scheme was used to maintain traceability. The results of this screening inspection are presented in Figs. 10a and 10b. Hot spot severity was qualitatively assigned as either 'significant' or 'less significant' based on how readily discernable they were by human operator review of the infrared images. Fig. 10a shows that within each 40 piece sample from the 7 lots tested there was at least 1 resistor and up to 6 resistors with a 'significant' hot spot. A total of 29 out 280 resistors were judged to have 'significant' hot spots with an additional 25 resistors having 'less significant' hot spots. Neither the type of foil used (i.e., Type A = with particles vs. Types B & C = "particle-free") nor the level of STOL screening (i.e., Types A & B = 1 STOL vs. Type C = 2 STOL exposures) appears to have produced a significant difference among the 7 lots tested in terms of number of resistors with hot spots remaining in the 40 piece samples.

a)

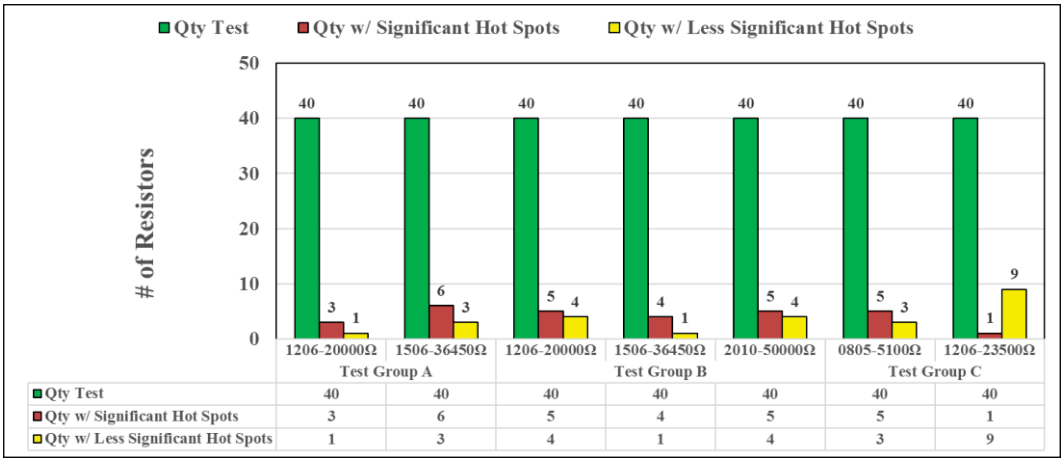

	1206-20000Ω	1506-36450Ω	1206-20000Ω	1506-36450Ω	2010-50000Ω	0805-5100Ω	1206-23500Ω
	Test Group A		Test Group B			Test Group C	
Qty Test	40	40	40	40	40	40	40
Qty w/ Significant Hot Spots	3	6	5	4	5	5	1
Qty w/ Less Significant Hot Spots	1	3	4	1	4	3	9

b)

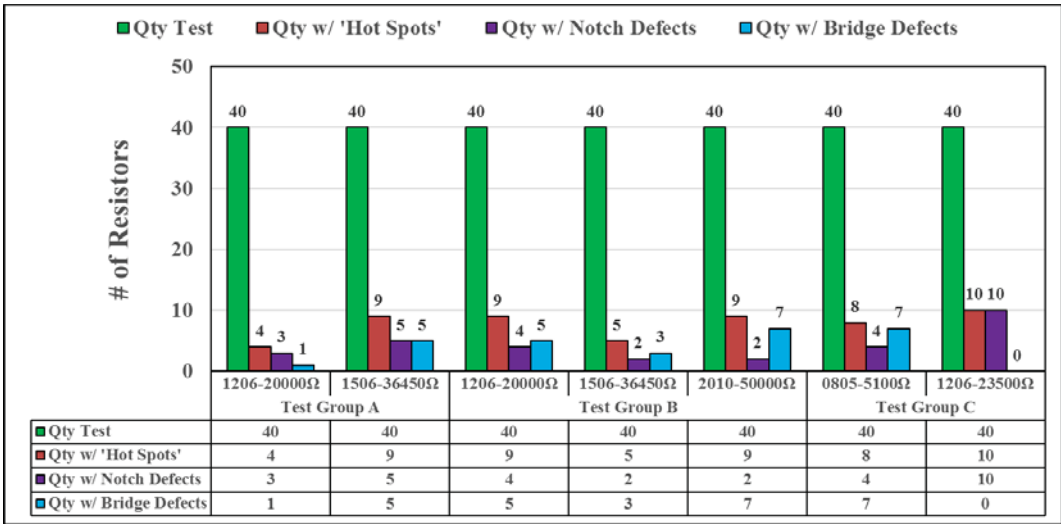

	1206-20000Ω	1506-36450Ω	1206-20000Ω	1506-36450Ω	2010-50000Ω	0805-5100Ω	1206-23500Ω
	Test Group A		Test Group B			Test Group C	
Qty Test	40	40	40	40	40	40	40
Qty w/ 'Hot Spots'	4	9	9	5	9	8	10
Qty w/ Notch Defects	3	5	4	2	2	4	10
Qty w/ Bridge Defects	1	5	5	3	7	7	0

Fig. 10 – Pre-Life Test Pulsed-Power Infrared Inspection Test Results by
a) Severity of Hot Spots and
b) Type of Hot Spots (Notches vs. Bridges)

Fig. 10b presents the same pre-life test pulsed-power infrared inspection results in terms of the total number of resistors with hot spots (total = ‘significant’ plus ‘less significant’) and then identifies them by the type of constriction defect (notch vs. bridge). Several resistors had more than one hot spot within the resistor pattern including some resistors having both notch and bridge type defects. For this reason the total number of resistors with hot spots does not always equal the sum of resistors with notches plus resistors with bridges.

Obviously, notch type defects present higher risk to resistors with narrower gridlines (i.e., higher resistance values) compared to ones with wider gridlines (i.e., lower resistance values) due to the increased potential for the notch to create a significant constriction defect. This fact makes it tempting to exempt lower value resistors from an enhanced screen of the type described herein. However, the potential impact of bridge defects, which are prevalent in every lot tested herein, is not affected very much by the gridline geometries and therefore, it remains of interest to consider an enhanced screen for bridge defects regardless of resistance value.

Life Test Results

After screening per the above infrared technique, all 280 resistors, including those with hot spots, were returned to the manufacturer for long-term life test. The resistors were assembled by the manufacturer onto printed wiring boards (PWBs) as shown in Fig. 11 using recommended practices (e.g., appropriate reflow profile, SnPb solder). Initial resistance was measured after PWB assembly to verify all resistors were initially within the expected tolerances shown in Table 3. All interim resistance measurements during the course of life test were made using a 4-wire Kelvin technique to ensure accuracy of measurements for these precision tolerance resistors.

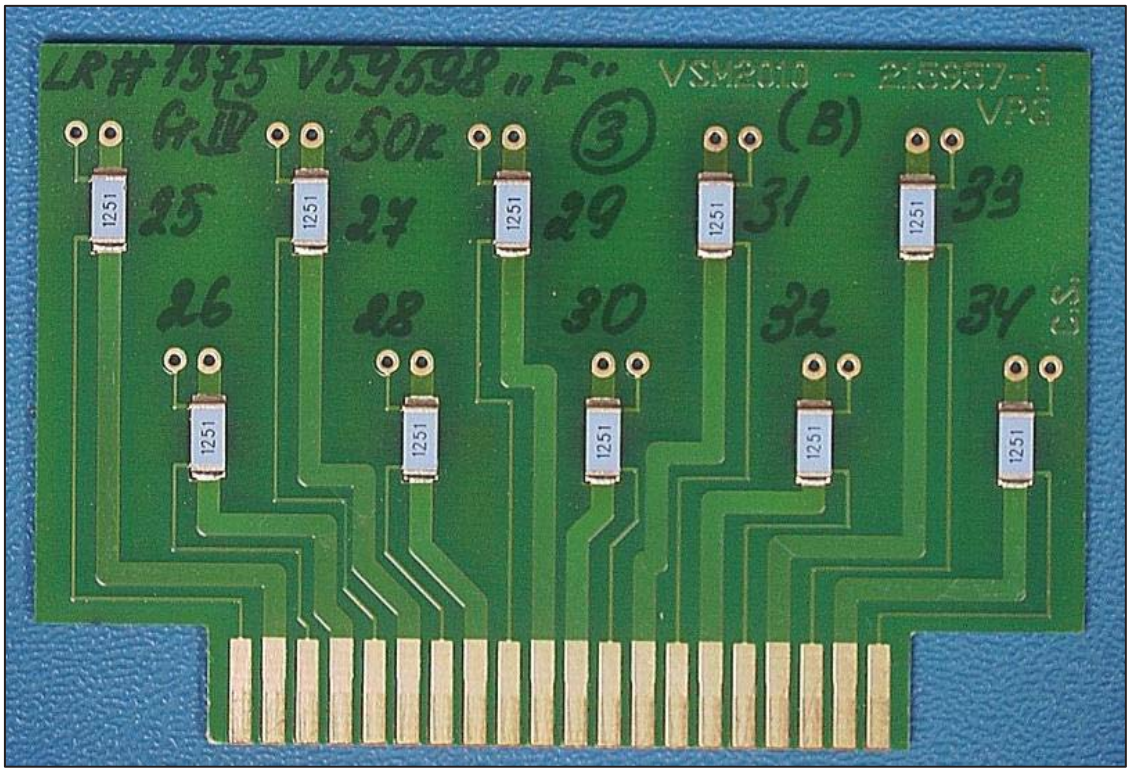

Fig. 11 – Example of Life Test PWB Used in this Evaluation (size 2010 resistors shown)

Life test was performed using the conditions in Table 4.

Table 4. Life Test Conditions.

Power Applied	**1x rated power** **Cycled 90 minutes on / 30 minutes off**
Test Temperature	**70°C**
Duration	**10,000 hours**
Interim Resistance Measurements	**250, 500, 1000, 2000, 4000, 6000, 8000 and 10000 hours**
Failure Criteria	**ΔR > ± 300 ppm**

During the course of life test 3 out of 280 resistors experienced positive resistance changes in excess of the rejection criteria of ΔR > ±300 ppm. Prior to life test the pulsed-power infrared inspection had identified 'significant' hot spots associated with bridge defects in each of the 3 resistors that failed during life test. All of the remaining 277 resistors performed within the specified life test criteria throughout test. Table 5 summarizes the actual resistance changes measured in parts per million (ppm) during life test and the number of hours of life test at which each failure was observed.

The three failures were from three different lots and each was from a different one of the three Types A, B and C. Failure conditions ranged from +4221 ppm to +19396 ppm changes in resistance. One of the three failures, S/N 12 of the 0805 - 5.1kΩ test group, actually experienced two distinct positive resistance shifts during life test each of which on its own would constitute failure. The first shift (+10440 ppm) was observed at the 250 hour inspection interval and then the second shift (an additional +925 ppm) was observed at 2000 hours of test. The other two life test failures were identified at the 4000 hour inspection interval. All failures were judged to be abrupt changes in resistance rather than gradual increases over time on test. Abrupt positive resistance changes such as these are consistent with fracture of bridge type defects within the active region of the resistor.

Table 5. 10,000 Hour Life Test Resistance Changes for 3 Failures
Italics Are Used to Identify Resistance Changes in Excess of Failure Criteria

Resistor Size, Value, S/N Type	**Change in Resistance from Initial Measurement (ppm)** **Failure Criteria ΔR > 300 ppm**							
	Hours of Life Test							
	250	**500**	**1000**	**2000**	**4000**	**6000**	**8000**	**10000**
0805, 5.1kΩ, S/N 12 Type "C"	****10440***	***10493***	***10550***	*****11365***	***11182***	***11209***	***11199***	***11195***
1206, 20kΩ, S/N 28 Type "A"	98	131	176	241	***19349***	***19477***	***19391***	***19396***
2010, 50kΩ, S/N 48 Type "B"	43	64	94	126	***4160***	***4192***	***4226***	***4221***

** S/N 12 exhibits 1st positive resistance shift in excess of failure criteria*
*** S/N 12 exhibits 2nd positive resistance shift in excess of failure criteria*

Post-Life Test Pulsed-Power Infrared Screening Results

At the conclusion of life test all 280 resistors were re-examined using the pulsed-power infrared inspection technique to identify any changes from the pre-life test observations. The 277 resistors (including 26 with significant hot spots) that passed life test with ΔR < 300 ppm each presented no changes in its infrared signature before vs. after life test. These observations are consistent with the constriction defects is these particular resistors remaining intact throughout life test and therefore, not exhibiting abrupt significant shifts in resistance.

The pre-life test and post-life test infrared images for each of the three life test failures are shown in Fig. 12. These comparison images show that each of these three resistors had 'significant' hot spots identified prior to life test and by the conclusion of life test either 1 or 2 bridge defects per resistor had lost electrical conductivity as evidenced by the disappearance of the hot spots in the post-life test infrared images.

Since S/N 12 (0805 - 5.1kΩ) exhibited two distinct and large positive resistance shifts (see Table 5), it is a good example to discuss the correlation between the resistance shifts and the infrared signature changes during life test. Fig. 12a shows that prior to life test S/N 12 contained 4 distinct hot spots each consisting of a bridge defect between adjacent gridlines. After life test, only 2 of the original 4 hot spots remained indicating that the other 2 bridge defects had become electrically open (i.e., non-conducting) during life test. As described earlier, the disruption of a bridge defect results in a positive resistance shift due to the removal of the parallel resistance pathway created by the bridge.

In the next section failure analyses of the 3 life test failures will provide further evidence that the observed positive resistance shift failure modes are due to fractured bridge defects in the resistor pattern.

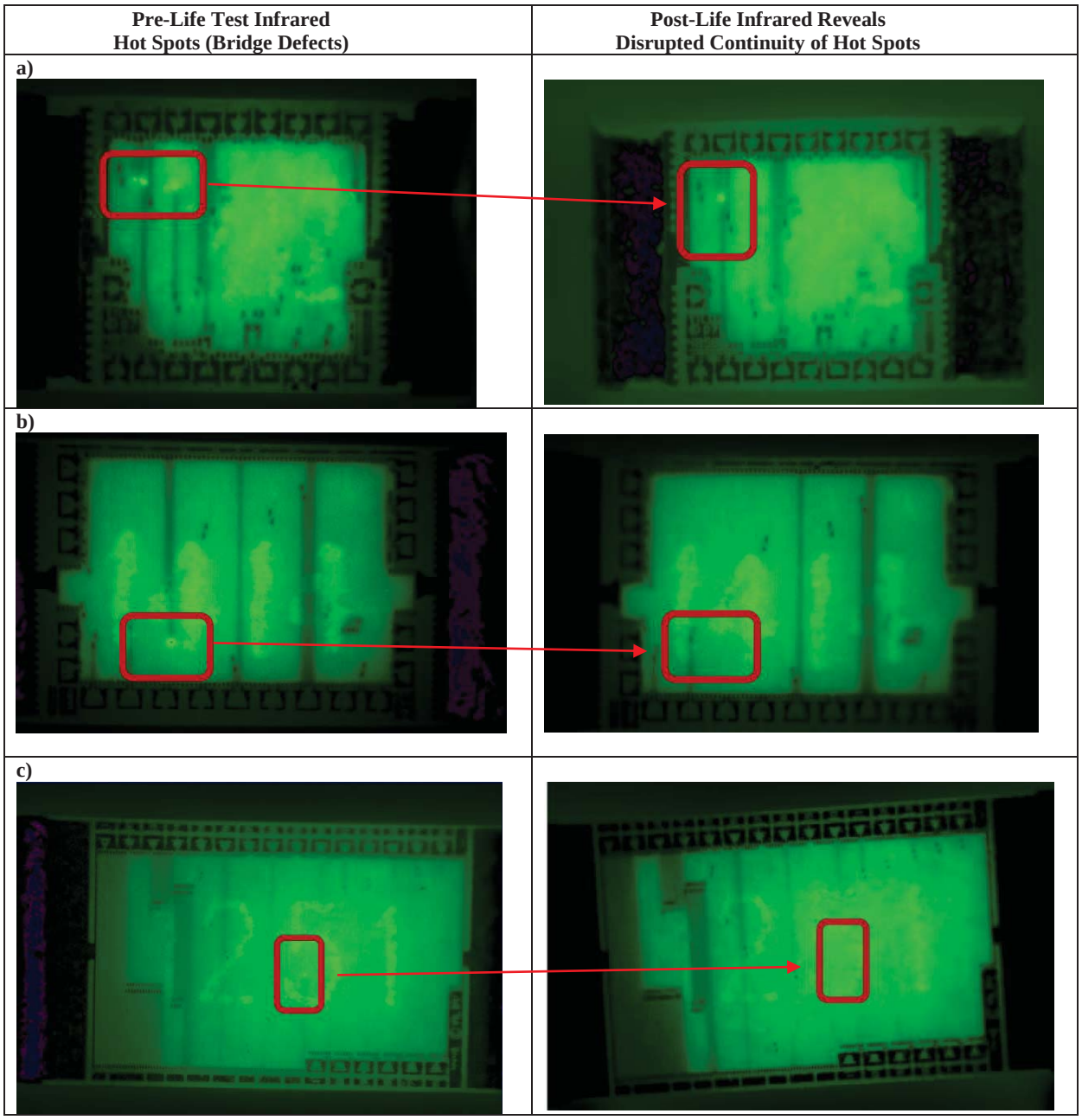

Fig. 12. Pre-Life Test and Post-Life Test Infrared Comparison Images of the Three Life Test Failures
a) Size 0805, 5.1kΩ, S/N12, Type C,
b) Size 1206, 20kΩ, S/N 28, Type A,
c) Size 2010, 50kΩ, S/N 48, Type B

FAILURE ANALYSES

Each of the three life test failures plus one passing resistor from each of these same three lots was subjected to destructive failure analysis. The resistors were desoldered from their life test boards using hot air techniques to minimize thermal stresses. External visual inspection with a low magnification stereo microscope revealed no anomalies. The resistors were deprocessed first with Dynasolve 2000 at ~100°C to remove the blue epoxy coating. Exposure times ranging from 6 to 18 minutes were used on the different resistors in order to completely remove the blue epoxy coatings. Rinsing was performed with water followed by acetone.

High magnification optical microscopy inspection using bright-field and dark-field illumination was performed after the blue epoxy coat removal. Transmitted light inspection (i.e., illuminating the sample from below and through the alumina substrate) was also used for all three resistors.

The resistors were then further deprocessed using reactive ion etching (RIE) with oxygen plasma to remove the translucent polymer protective coating thus exposing the nichrome alloy foil resistor element. Cumulative plasma etch times ranged from 30 to 135 minutes per resistor. Interim inspections were performed during RIE to assess progress of the polymer coating removal in order to prevent over-etching which could result in removal of the adhesive that bonds the etched foil resistor element to the alumina substrate. After sufficient removal of the polymer coating over the foil resistor pattern, each resistor was examined via SEM and energy dispersive X-ray spectroscopy (EDS) to document the conditions of suspected bridge defect disruptions.

The results of these inspections are shown in Figs. 13 and 14. Fig. 13a shows the pre-life test infrared image of a resistor that had 4 significant hot spots each associated with a bridge defect. Fig. 13b is an optical microscopy image of the same resistor after removal of the opaque epoxy coating. Optical inspection through the translucent polymer coating that protects the resistor element shows certain aspects of these 4 bridge defects. However, especially at higher magnifications, factors such as focal range and optical reflections from the complicated shapes of the constrictions make it exceedingly difficult to quantify the dimensions of such defects. Fig. 13c shows a SEM view of the same region from Fig. 13b after complete removal of the polymer coating. The SEM, with its superior focal depth and magnification capabilities, reveals enhanced details of constriction defects not possible with optical microscopy.

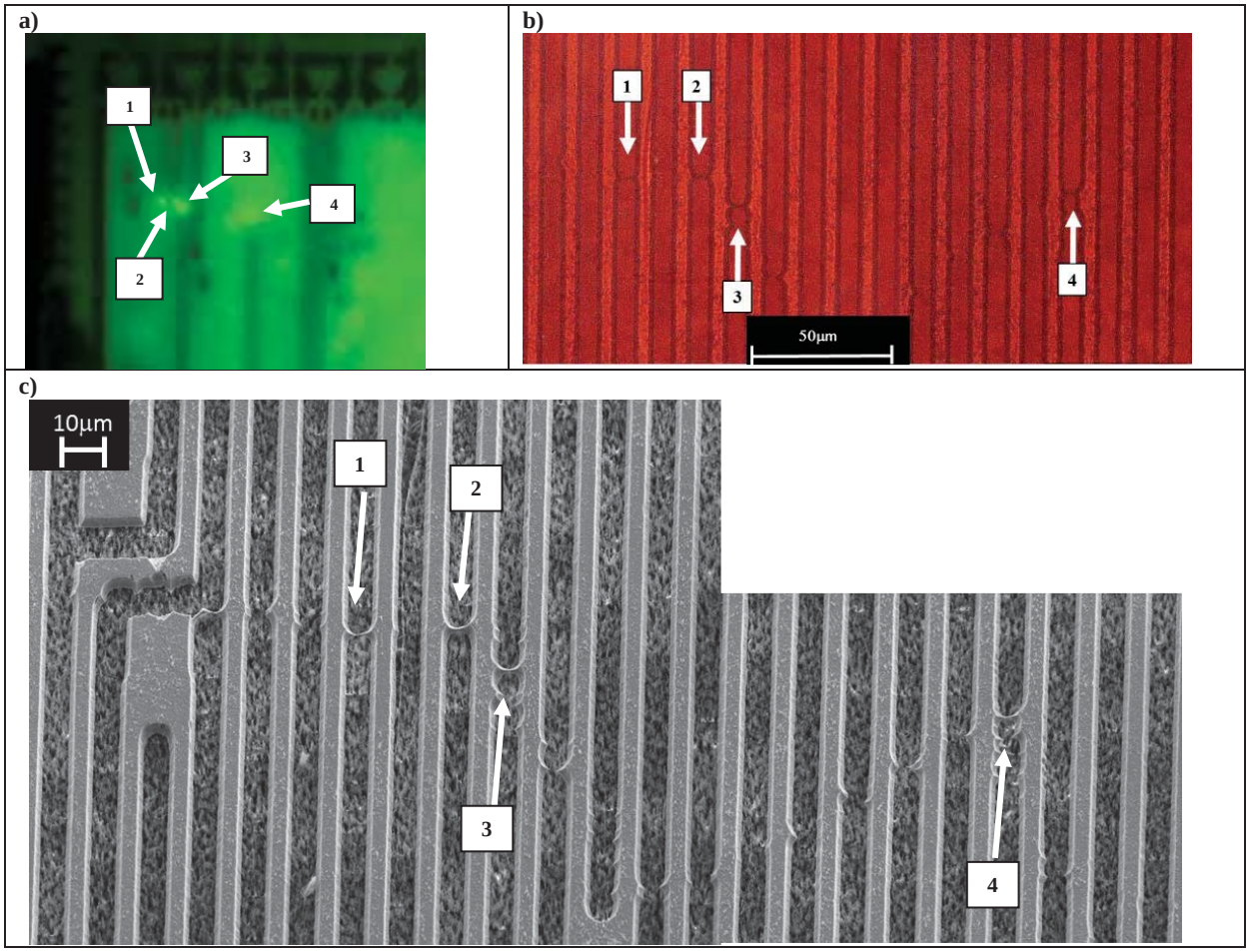

Fig 13. Failure Analysis Size 0805, 5.1kΩ, S/N 12
a) Infrared Image Showing 4 Hot Spots Associated with Bridge Defects
b) Transmitted Light Microscopy Montage Image Highlighting Bridge Defects in a),
c) SEM Image of Region Shown in b)

Fig. 14 shows that the failure sites for all 3 life test failures were identified and confirmed to be fractured bridge defects consistent with the locations of the pre-life test hot spots that had disappeared at discrete time intervals during life test. Each of these previously-conducting bridge defects fractured at the approximate mid-point in their span producing an open circuit condition in the bridge. The fractured bridges resulted in the removal of parallel resistance pathways in each resistor pattern thus producing the observed positive resistance shift failure modes. Detailed inspection of the fractured bridges shows no evidence of melting nor tensile stretch-to-break failure. Instead, the fractures are all consistent with cyclical fatigue fracture. The source of cycling was thermomechanically-induced by the on/off power cycling that resulted in hot spot expansion and contraction during the life test.

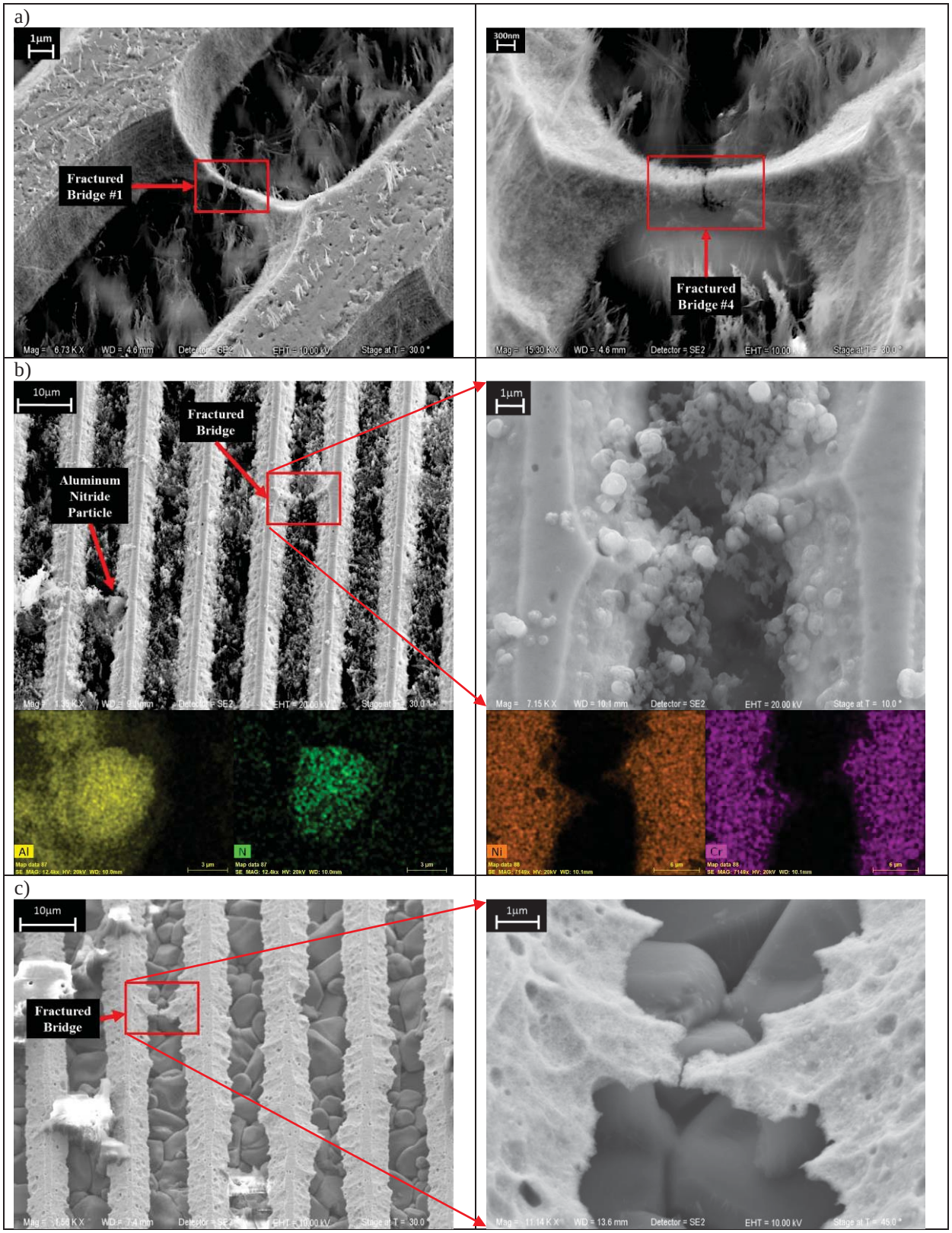

Fig. 14 – SEM and EDS Images of Once-Conducting Bridge Defects that Fractured During Life Test
a) Size 0805, 5.1kΩ, S/N12, Type C, Showing the Fractured Bridges Labeled "1" and "4" in Fig. 13,
b) Size 1206, 20kΩ, S/N 28, Type A Fractured Bridge and EDS of an Embedded Aluminum Nitride Particle
c) Size 2010, 50kΩ, S/N 48, Type B, Fractured Bridge Defect

Three resistors with significant hot spots that persisted after life test were also deprocessed as described above to enable detailed SEM inspection (see fig. 15). High magnification SEM inspection of these three resistors showed evidence of emerging (fig. 15a) and/or near-complete fracture of the constrictions associated with these hot spots. In particular figs. 15b and 15c show evidence of near-complete fracture of the constriction. It is possible resistors in this condition will exhibit intermittent resistance changes caused by small displacements of the fractured ends that make and break pressure contact between the ends of the constriction. Such displacements may be produced by changes in ambient temperature leading to expansion and contraction of the resistor materials. Intermittent behavior like this would be very difficult to detect during life test since continuous resistance monitoring is not used.

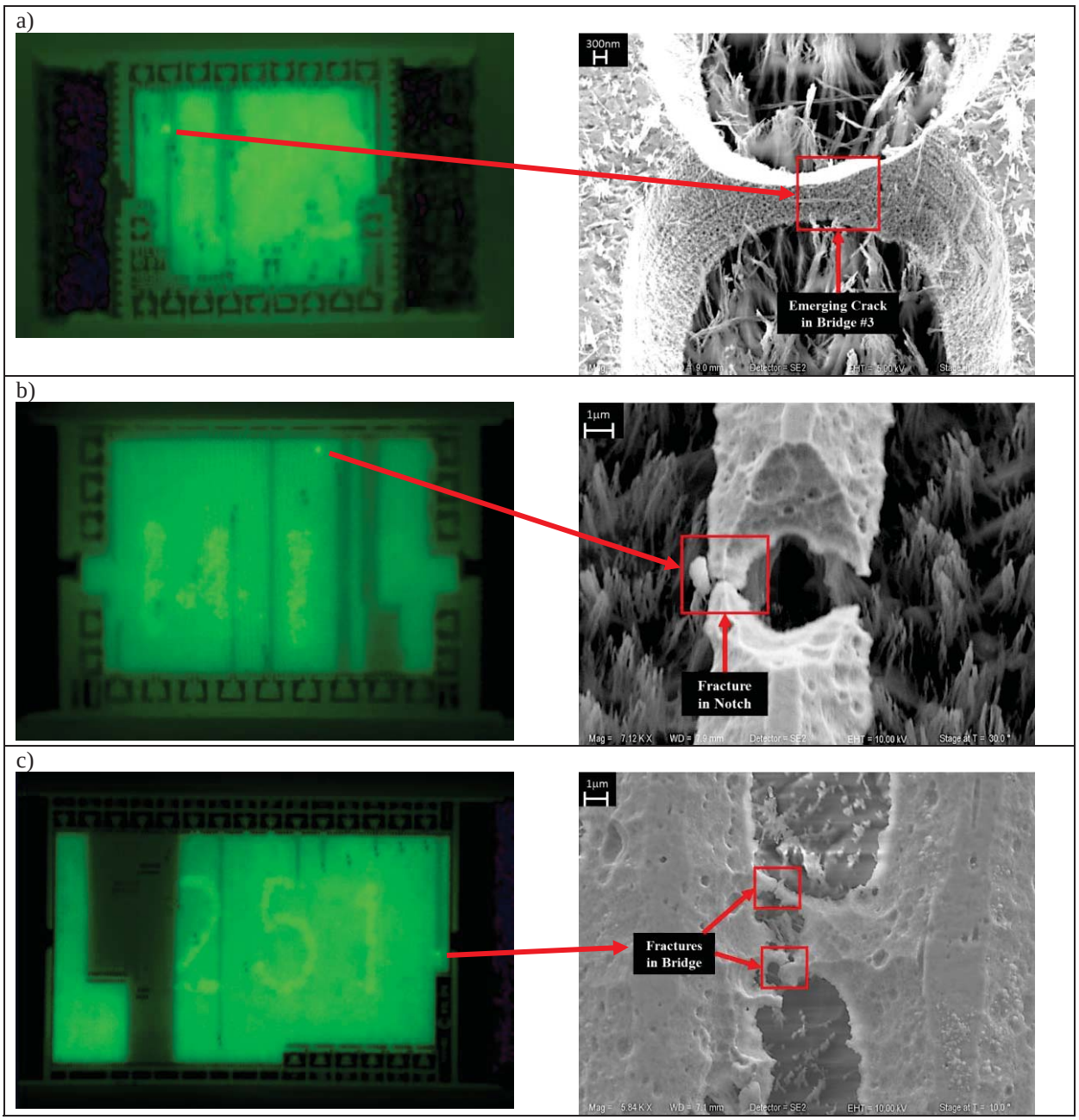

Fig. 15. Infrared and Corresponding SEM Images of Constriction Defects that Remained Intact Through Life Test
a) Size 0805, 5.1kΩ, S/N12, Type C, Bridge Defect (see Fig. 13 bridge #3) with Emerging Fracture
b) Size 1206, 20kΩ, S/N 25, Type A, Notch Defect with Near-Complete Fracture
c) Size 2010, 50kΩ, S/N 33, Type B, Bridge Defect with Two Near-Complete Fractures

CONCLUSIONS

Bulk metal foil and thin film resistors are occasionally produced having localized constriction defects (e.g., notches and bridges) within the active region of the etched resistor pattern. These types of defects have occasionally been observed to break in service (and during life test) due to the formation of localized hot spots that, especially during power cycling, result in thermomechanically-induced fatigue fracture. The severity of failure depends on the type (notch vs. bridge) and location of the constriction in the pattern, but the failure mode is always a positive resistance change up to and including open circuit failure. Resistance shifts due to fracture of constriction defects can be permanent or intermittent. Intermittent resistance changes may occur if the fractured constriction defect undergoes displacements sufficient to make or break contact between the severed ends. Past experiences with this type of resistor include intermittent failures which abruptly, repeatedly and reversibly changed resistance at particular ambient temperatures.

Traditional resistor inspection techniques such as pre-encapsulation visual inspection, short time overload (STOL), power conditioning, and lot sample workmanship inspection via DPA can identify many resistors with constriction defects, but they do not remove all resistors with constrictions that may fracture in service. To augment these traditional inspections, a new screening inspection technique has been developed using a FLIR SC8300 high speed, high resolution infrared camera and 4x lens while applying 1 or more brief power pulses (e.g., 50 ms @ 6.25x rated power) to the resistor under test. Resistors with significant localized constriction defects in the resistor pattern exhibit hot spots during this infrared inspection. Feature sizes below 5μm are readily detectable with this technique.

A conservative rejection criteria is to remove from the lot any resistor that exhibits a hot spot. This technique has been demonstrated to be usable as a non-destructive, post-procurement screening inspection on surface mount foil resistors and thin film resistors where the specific coatings used to protect the resistor element are highly transmissive in the spectral range of the infrared detector employed. Ideally, this same technique could be incorporated as an in-process screening inspection by a resistor manufacturer after resistor trimming to final value and prior to encapsulation.

To assess the effectiveness of this pulsed-power infrared screening technique, we obtained a total of 280 high resistance value surface mount foil resistors comprised of 40 resistors from each of 7 different production lots. All of the resistors were pre-screened by the manufacturer using 100% pre-encapsulation visual inspection of the resistor pattern followed by either 1 or 2 exposures to STOL to remove as many defective resistors as these tests may detect. Next, the pulsed-power infrared inspection test described herein was performed during which 29 resistors were identified with significant hot spots associated with 1 or more notch and/or bridge defects in the resistor pattern. Resistors with hot spots were found at approximately the same rates of occurrence in each of the 7 lots regardless of the level of manufacturer pre-screening (e.g., 1 vs. 2 STOL exposures).

After the infrared screening test, all 280 resistors, including those with hot spots, were subjected to an industry standard 10000 hour life test at 1x rated power at 70°C with power cycled on for 90 minutes and off for 30 minutes. During the life test 3 resistors with significant hot spots prior to life test exhibited one or more positive resistance shift failure modes ranging from ~4000 ppm to ~19000 ppm detected after 250, 2000 and 4000 hours. Post-life test infrared inspection revealed that 1 or 2 pre-life test hot spots had disappeared from each of the 3 life test failures. The 277 resistors that passed life test all exhibited no changes in their infrared signatures before vs. after life test.

The 3 life test failures plus a few additional resistors that passed life test were then subjected to destructive analyses using a two-step chemical and plasma etching deprocessing scheme to remove the protective coating materials. High magnification inspection using SEM and EDS confirmed that each of the 3 life test failures had either 1 or 2 previously-conducting bridge defects that fractured at the approximate mid-point in their span producing an open circuit condition in the bridge. Each fractured bridge resulted in the removal of a parallel resistance pathway in the resistor pattern thus producing the observed positive resistance shift failure modes. Detailed inspection of the fractured bridges showed no evidence of melting nor tensile stretch-to-break failure of the bridge. Instead, the fractures are consistent with cyclical fatigue fracture. It is concluded that the repetitive on/off power cycling during life test resulted in localized, thermomechanical expansion and contraction of the bridge defects (i.e., one expansion/contraction per on/off power cycle) that eventually caused the bridges to fracture. SEM analyses of resistors with significant hot spots that passed life test showed evidence of emerging and/or near-complete fracture of their constriction defects. Since continuous resistance monitoring was not used during life test, it is possible some of these resistors exhibited intermittent resistance changes resulting from small displacements between the fractured ends of the constrictions causing them to make and break pressure contact between the fractured ends.

For applications requiring the highest reliability foil or thin film resistors, the authors recommend the use of the pulsed-power infrared screening technique described herein. This test can be adapted as an in-process manufacturing screen or as a post-procurement screening inspection. Both approaches identify resistors with localized constriction defects in the pattern. This evaluation and prior field experiences have shown such constriction defects have the potential to fracture in service resulting in positive resistance shift failure modes up to and including open circuits.

ACKNOWLEDGMENTS

The authors wish to acknowledge the NASA Electronic Parts & Packaging (NEPP) program and Mike Sampson for supporting this research. Special thanks is given to Jacob Musel, Ori Sinkevich and Steve Phillips of Vishay Precision Group for providing foil resistors and life testing services for this evaluation. Gratitude is given to Tim Mondy, Alexandros Bontzos, Matthew King-Smith, Henning Leidecker and Jack Shue at NASA Goddard Space Flight Center (GSFC) for their support in the development and implementation of the pulsed-power infrared screening technique. We are indebted to Chris Greenwell, Ron Weachock and Nilesh Shah of ASRC AS&D at NASA GSFC for their failure analysis expertise.

REFERENCES

[1] MIL-PRF-55342H with amendment 5, "Resistor, Chip, Fixed, Film, Nonestablished Reliability, Established Reliability, Space Level, General Specification for", Sept. 5, 2017

[2] Models 303133 through to 303138 (Ultra High Precision Surface Mount Chip Resistors, VSMP Z-Foil Technology Configuration), Vishay Precision Group Data Sheets, http://www.vishaypg.com/docs/63169/30313x.pdf

[3] MIL-PRF-55182H with amendment 3, "Resistors, Fixed, Film, Non-established Reliability, Established Reliability, And Space Level, General Specification For", Appendix B, para. B.7.2, April 8, 2009.

[4] NASA GSFC Code 562 Failure Analysis Report J17534FA, draft March 2018.

[5] NASA GSFC Code 562 Failure Analysis Report Q80471, March 6, 2009.

[6] NASA GSFC Code 562 Evaluation Report Q80487, March 13, 2009.

[7] NASA GSFC Code 562 Evaluation Report Q80490, April 3, 2009.

[8] NASA GSFC Code 562 Evaluation Report J12427, April 26, 2013.

[9] U.S. Patent 3,405,381, "Thin Film Resistor", Oct. 8, 1968, Felix Zandman, Branin Boyd, Vishay Intertechnology, Inc.

[10] U.S. Patent 4,378,549, "Resistive Electrical Components", Mar. 29, 1983, Joseph Szware, Ramat Gan, Vishay Intertechnology, Inc.

[11] MIL-PRF-1580B with change 3, "Destructive Physical Analysis for Electronic, Electromagnetic and Electromechanical Parts", para. 18.4.3, March 4, 2014.

[12] L. Panashchenko, J. Brusse, M. King-Smith, "A Screening Method Using Infrared Imaging to Detect Pattern Defects in Foil and Thin Film Resistors", *2015 Components for Military and Space Electronics (CMSE) Conference and Exhibition*, Los Angeles, CA, March 1-3, 2015.

[13] FLIR SC8000 series data sheet, http://www.flirmedia.com/MMC/THG/Brochures/RND_018/RND_018_US.pdf